Supplementary Information

Influence of a sublayer structure of thin-film composite reverse osmosis membranes on the overall water flux

Jaewoo Lee[a,b,c], Hongsik Yoon[a], Jae Hyun Yoo[a], Dong-Chan Choi[a], Chang H. Nahm[a], Sang Hyun Lee[a], Hee-Ro Chae[a], Yong Hyup Kim[b], Chung-Hak Lee[a,*], and Pyung-Kyu Park[d,]**

[a] School of Chemical and Biological Engineering, Seoul National University, 1 Gwanak-ro, Gwanak-gu, Seoul 08826, Republic of Korea

[b] School of Mechanical and Aerospace Engineering, Seoul National University, 1 Gwanak-ro, Gwanak-gu, Seoul 08826, Republic of Korea

[c] BK21 Plus Transformative Training Program for Creative Mechanical and Aerospace Engineers, Seoul National University, 1 Gwanak-ro, Gwanak-gu, Seoul 08826, Republic of Korea

[d] Department of Environmental Engineering, Yonsei University, 333 Baekun Hall, 1 Yonseidae-gil, Wonju, Gangwon-do 26493, Republic of Korea

*E-MAIL: leech@snu.ac.kr, TEL: +82-2-880-7075, FAX: +82-2-874-0896

**E-MAIL: pkpark@yonsei.ac.kr, TEL: +82-33-760-2890

1

Results and Discussion

Correlation between the active layer characteristics and the performance of TFC RO membranes consisting of support layers with distinct structures

Different characteristics of the support layers can induce the different active layer characteristics such as roughness and thickness by changing the diffusion rate of MPD[1] and consequently the formation of an active layer with a different permeability, resulting in differences in RO performance. Thus, we first examined the correlation between the active and support layer characteristics of the as-prepared TFC membranes regarding the thickness, roughness, and the degree of cross-linking of the active layer, as has been discussed previously by Lee.[2] The above three characteristics are known to affect the RO flux.[3-5] Also, the contact angle was measured to determine the surface chemistry effect of the active layer on the water permeability of an RO membrane. Although surface pore size significantly decreased with increasing polymer concentration (Fig. 5), there was no discernible difference in the three kinds of active layer characteristics which are known to be able to change with the tendency of MPD diffusion[5] (Figs. S3(a) to (c)). From these data, we can discern that the surface pores, ranging from 4.5 nm to 6.7 nm, have no significant difference in the view of the MPD diffusion. Lastly, there was also no relationship between the contact angle and the type of support layer (Fig. S3(d)), which was understandable given that all the TFC membranes were fabricated using the same chemicals and methods.

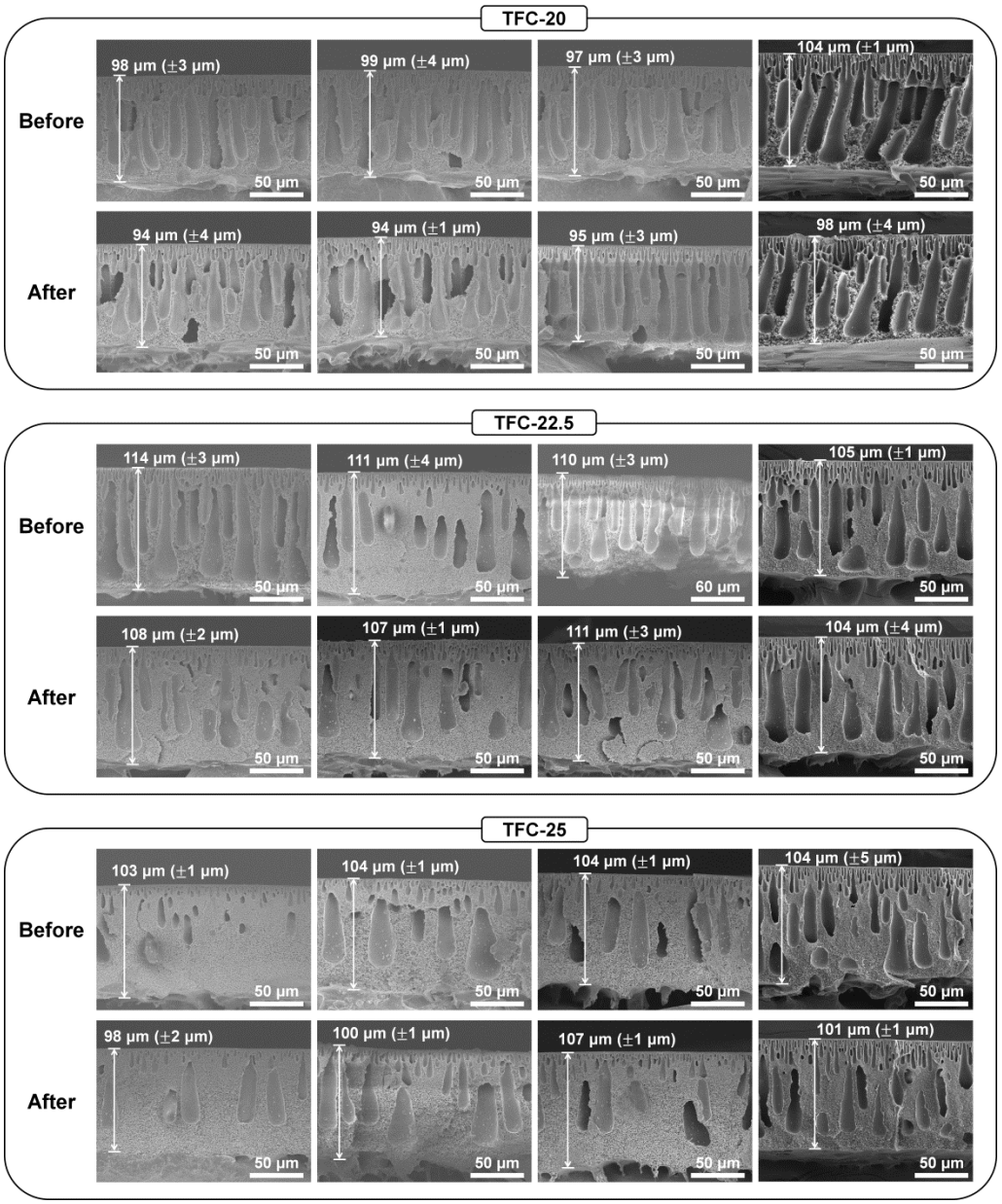

Fig. S1. SEM images to verify changes in the support layer morphology arising from membrane compaction. According to the previous literature,[6] the degree of membrane deformation by compaction can be indirectly evaluated by measuring the thickness of the support layer after RO operation. Accordingly, the thicknesses of arbitrarily chosen locations were measured after membrane compaction at 2,500 kPa for 30 min and at 1,500 kPa for another 30 min. According to the statistical analysis, there was no discernible difference in the support layer thickness before and after membrane compaction, regardless of the sample type (see Table S1 for statistical analysis).

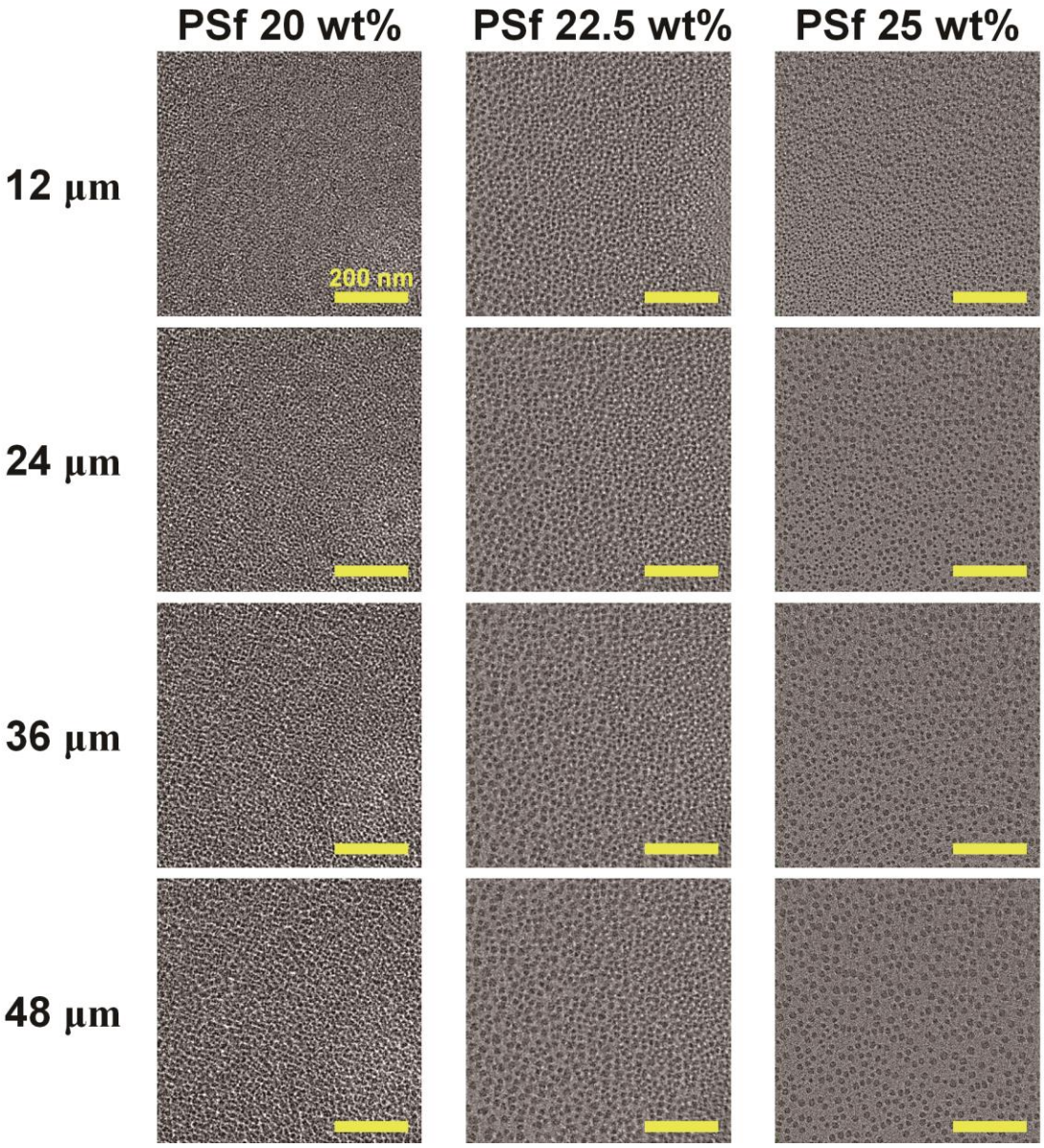

Fig. S2. Tomograms of the support layers obtained at different heights by non-destructive inspection.

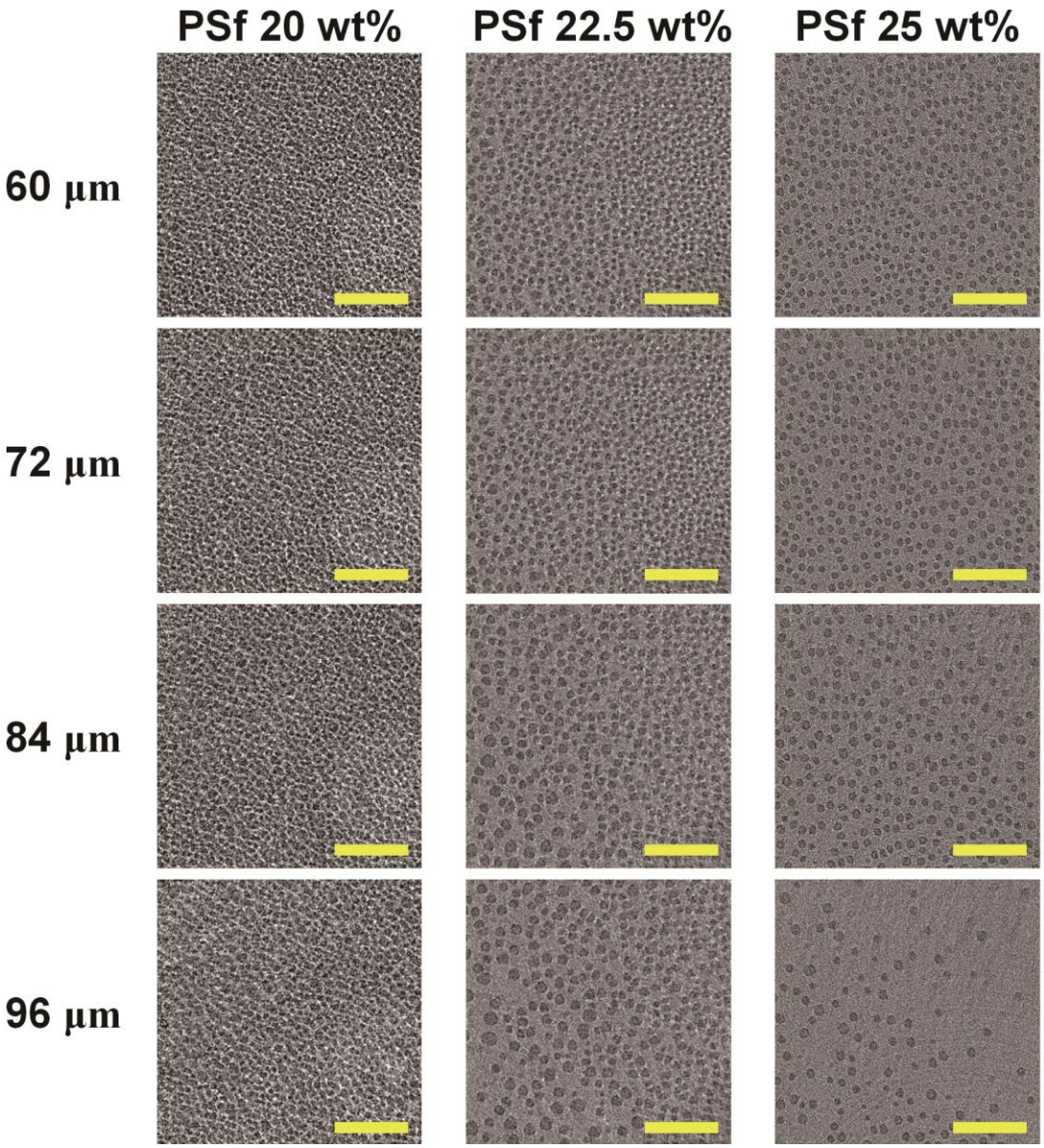

Fig. S2. (Continued)

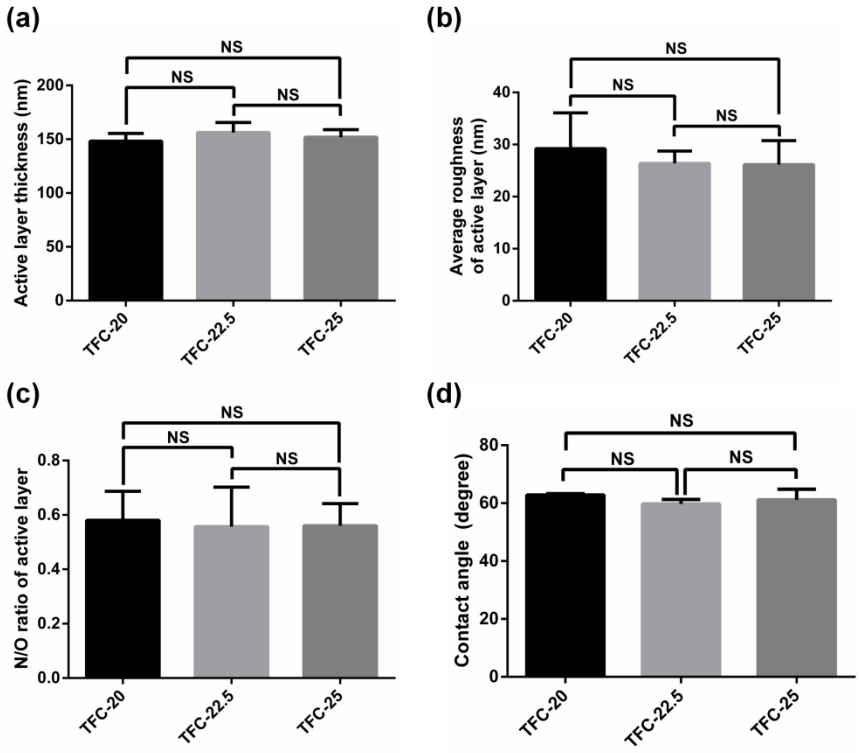

Fig. S3. (a) The average thickness of each active layer. See more detail in Fig. S4 and Table S9 for statistical analysis. Error bars indicate the standard deviations obtained from three different samples. (b) Average roughness and (c) nitrogen/oxygen (N/O) ratio of each active layer. For more detail, see Fig. S5 for the average roughness and Tables S10 and S11 for statistical analysis. Error bars indicate the standard deviations obtained from four and three different samples for the average roughness and the N/O ratio, respectively. (e) Contact angle of each active layer. Error bars indicate the standard deviations obtained from five different samples. See more detail in Table S12 for statistical analysis. One-way ANOVA and Tukey's post-tests were performed to compare each data where significant differences are indicated as follows: NS (not significant) $P > 0.05$.

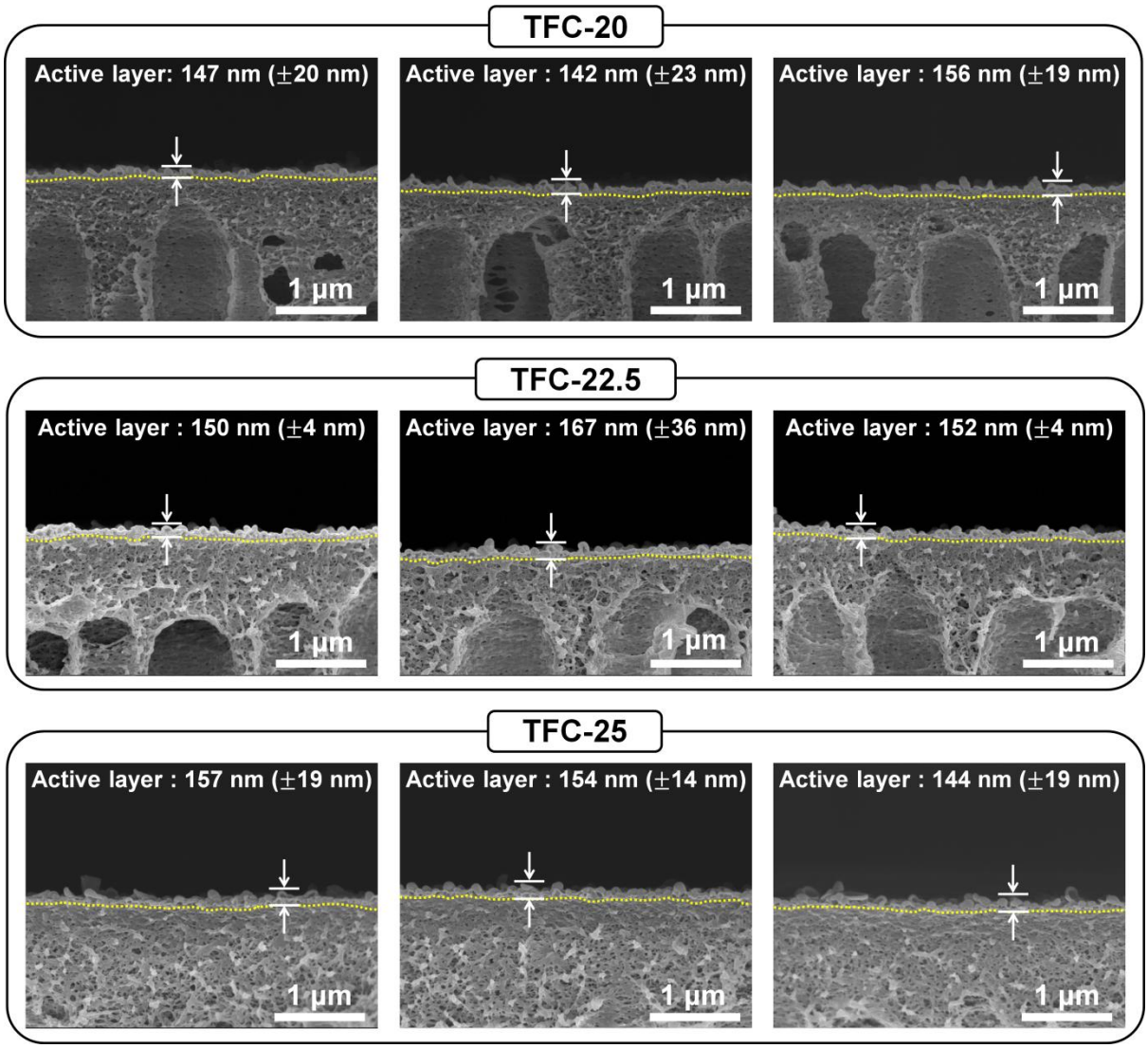

Fig. S4. Cross-sectional SEM images of TFC-20, TFC-22.5, and TFC-25 membranes with the average thicknesses of their active layer. The number in parentheses is the standard deviation obtained at five arbitrary locations.

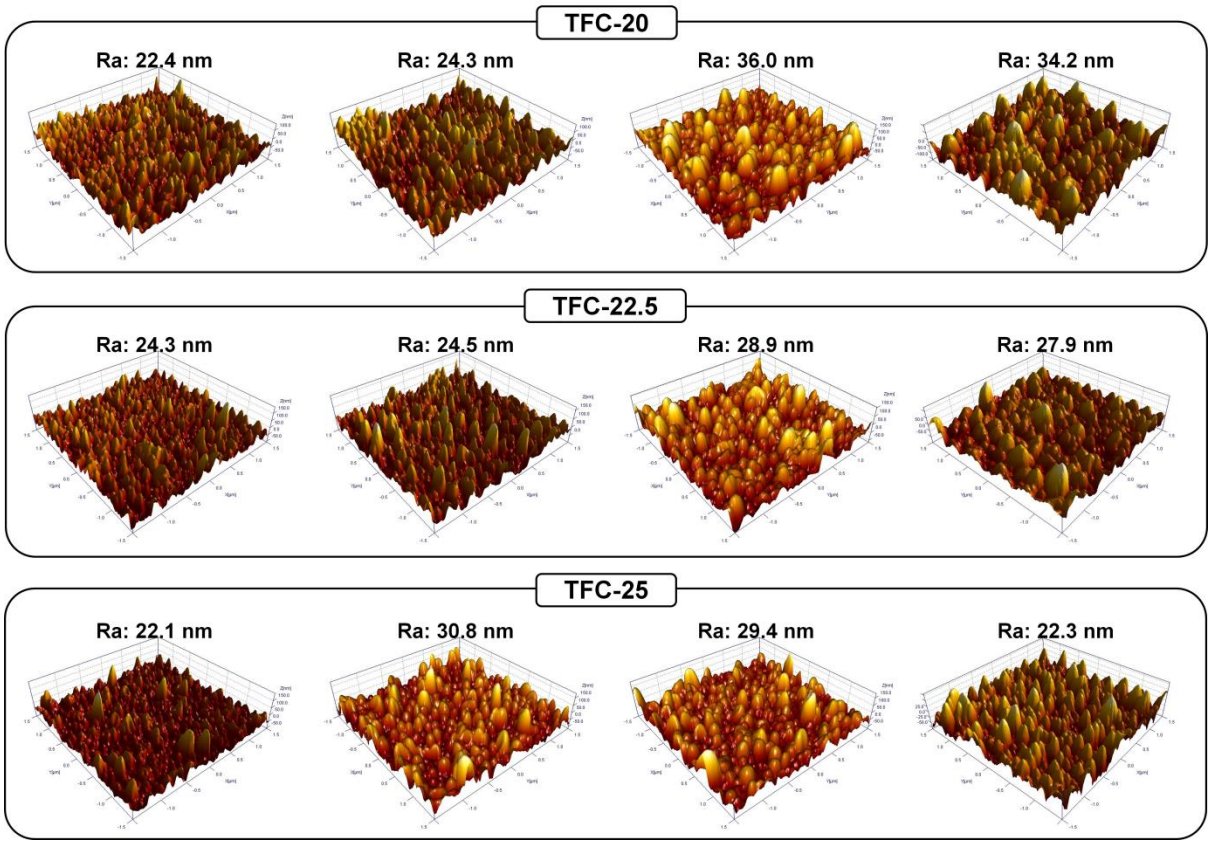

Fig. S5. AFM images of active layers of TFC-20, TFC-22.5, and TFC-25.

Table S1. Differences between the support layer thicknesses before and after membrane compaction as determined by Student's *t*-test. Significant differences are indicated as follows: NS (not significant) P > 0.05, * P < 0.05, ** P < 0.01, *** P < 0.001 and **** P < 0.0001.

Sample	Significant? P < 0.05?	Summary	P Value
TFC-20	No	NS	0.0531
TFC-22.5	No	NS	0.2901
TFC-25	No	NS	0.2850

Table S2. Differences between water fluxes of the TFC-20, TFC-22.5, and TFC-25 membranes as determined by one-way analysis of variance (ANOVA) with Tukey's multiple comparison test: mean difference, 95% CI of the difference, and adjusted P value. In Graph Pad Prism 6 software, significant differences are indicated as follows: NS (not significant) P > 0.05, * P < 0.05, ** P < 0.01, *** P < 0.001 and **** P < 0.0001.

Comparison test	Mean Diff.	95% CI of diff.	Significant? P < 0.05?	Summary
TFC-20 vs. TFC-22.5	13.49	6.717 to 20.26	Yes	***
TFC-20 vs. TFC-25	16.88	10.11 to 23.65	Yes	****
TFC-22.5 vs. TFC-25	3.391	-3.380 to 10.16	No	NS

Table S3. Differences between salt rejections of the TFC-20, TFC-22.5, and TFC-25 membranes as determined by one-way analysis of variance (ANOVA) with Tukey's multiple comparison test: mean difference, 95% CI of the difference, and adjusted P value. In Graph Pad Prism 6 software, significant differences are indicated as follows: NS (not significant) P > 0.05, * P < 0.05, ** P < 0.01, *** P < 0.001 and **** P < 0.0001.

Comparison test	Mean Diff.	95% CI of diff.	Significant? P < 0.05?	Summary
TFC-20 vs. TFC-22.5	0.3425	-0.3262 to 1.011	No	NS
TFC-20 vs. TFC-25	0.6406	-0.02803 to 1.309	No	NS
TFC-22.5 vs. TFC-25	0.2981	-0.3705 to 0.9668	No	NS

Table S4. Differences between tensile strengths of the TFC-20, TFC-22.5, and TFC-25 membranes as determined by one-way analysis of variance (ANOVA) with Tukey's multiple comparison test: mean difference, 95% CI of the difference, and adjusted P value In Graph Pad Prism 6 software, significant differences are indicated as follows: NS (not significant) P > 0.05, * P < 0.05, ** P < 0.01, *** P < 0.001 and **** P < 0.0001.

Comparison test	Mean Diff.	95% CI of diff.	Significant? P < 0.05?	Summary
TFC-20 vs. TFC-22.5	-1.950	-3.112 to -0.7885	Yes	**
TFC-20 vs. TFC-25	-2.418	-3.580 to -1.256	Yes	***
TFC-22.5 vs. TFC-25	-0.4675	-1.629 to 0.6943	No	NS

Table S5. Differences between moduluses of the TFC-20, TFC-22.5, and TFC-25 membranes as determined by one-way analysis of variance (ANOVA) with Tukey's multiple comparison test: mean difference, 95% CI of the difference, and adjusted P value In Graph Pad Prism 6 software, significant differences are indicated as follows: NS (not significant) $P > 0.05$, * $P < 0.05$, ** $P < 0.01$, *** $P < 0.001$ and **** $P < 0.0001$.

Comparison test	Mean Diff.	95% CI of diff.	Significant? $P < 0.05$?	Summary
TFC-20 vs. TFC-22.5	-42.41	-101.3 to 16.51	No	NS
TFC-20 vs. TFC-25	-126.6	-185.5 to -67.67	Yes	***
TFC-22.5 vs. TFC-25	-84.19	-143.1 to -25.26	Yes	**

Table S6. Differences between mean surface pore sizes of the PSf-20, PSf-22.5, and PSf-25 membranes as determined by one-way analysis of variance (ANOVA) with Tukey's multiple comparison test: mean difference, 95% CI of the difference, and adjusted P value In Graph Pad Prism 6 software, significant differences are indicated as follows: NS (not significant) P > 0.05, * P < 0.05, ** P < 0.01, *** P < 0.001 and **** P < 0.0001.

Comparison test	Mean Diff.	95% CI of diff.	Significant? P < 0.05?	Summary
TFC-20 vs. TFC-22.5	1.540	0.6925 to 2.388	Yes	**
TFC-20 vs. TFC-25	2.227	1.379 to 3.074	Yes	***
TFC-22.5 vs. TFC-25	0.6867	-0.1608 to 1.534	No	NS

85

86 Table S7. Reynolds numbers and variations derived experimentally.

Support layer	PSf-20	PSf-22.5	PSf-25
Specific surface area, S_v [m^{-1}, $n = 3$]	19.1×10^6 ($\pm 3.1 \times 10^6$)	26.4×10^6 ($\pm 5.0 \times 10^6$)	22.0×10^6 ($\pm 3.4 \times 10^6$)
Superficial velocity, v_s [m s^{-1}, $n = 5$]	13.0×10^{-6} ($\pm 1.8 \times 10^{-6}$)	8.7×10^{-6} ($\pm 0.5 \times 10^{-6}$)	7.6×10^{-6} ($\pm 1.3 \times 10^{-6}$)
Reynolds number, Re_p	4.1×10^{-6}	2.0×10^{-6}	2.1×10^{-6}

87

Table S8. Data for osmotic separation operations to estimate the pressure drop occurring in the support layer of the TFC-25 prepared without the additives.

Support layer	**PSf-25**
Tortuosity*, τ	174
Structure parameter, S	26,186
Specific surface area, S_v [m^{-1}, $n = 3$]	22.0×10^6 ($\pm 3.4 \times 10^6$)
Superficial velocity, v_s [m s^{-1}, $n = 5$]	2.1×10^{-6} ($\pm 0.3 \times 10^{-6}$)
Porosity, ε [$n = 3$]	0.67 (±0.02)
Intrinsic water permeability, A [L m^{-2} h^{-1} bar^{-1}, $n = 5$]	0.51 (±0.07)
Salt permeability, B [μm s^{-1}, $n = 5$]	0.04 (±0.01)
Salt rejection, R [%, $n = 5$]	97.7 (±0.6)
Water flux in FO mode, J_w^{FO} [L m^{-2} h^{-1}, $n = 3$]	1.04 (±0.10)

* Equations (4) and (5) were used to determine tortuosity with a diffusivity of 1.61×10^{-9} m^2 s^{-1} for NaCl [7].

Table S9. Differences between active layer thicknesses of the TFC-20, TFC-22.5, and TFC-25 membranes as determined by one-way analysis of variance (ANOVA) with Tukey's multiple comparison test: mean difference, 95% CI of the difference, and adjusted P value In Graph Pad Prism 6 software, significant differences are indicated as follows: NS (not significant) $P > 0.05$, * $P < 0.05$, ** $P < 0.01$, *** $P < 0.001$ and **** $P < 0.0001$.

Comparison test	Mean Diff.	95% CI of diff.	Significant? $P < 0.05$?	Summary
TFC-20 vs. TFC-22.5	-8.111	-27.93 to 11.71	No	NS
TFC-20 vs. TFC-25	-3.667	-23.48 to 16.15	No	NS
TFC-22.5 vs. TFC-25	4.444	-15.37 to 24.26	No	NS

Table S10. Differences between active layer roughnesses of the TFC-20, TFC-22.5, and TFC-25 membranes as determined by one-way analysis of variance (ANOVA) with Tukey's multiple comparison test: mean difference, 95% CI of the difference, and adjusted P value In Graph Pad Prism 6 software, significant differences are indicated as follows: NS (not significant) $P > 0.05$, * $P < 0.05$, ** $P < 0.01$, *** $P < 0.001$ and **** $P < 0.0001$.

Comparison test	Mean Diff.	95% CI of diff.	Significant? $P < 0.05$?	Summary
TFC-20 vs. TFC-22.5	2.825	-6.967 to 12.62	No	NS
TFC-20 vs. TFC-25	3.075	-6.717 to 12.87	No	NS
TFC-22.5 vs. TFC-25	0.2500	-9.542 to 10.04	No	NS

Table S11. Differences between N/O ratios of the TFC-20, TFC-22.5, and TFC-25 membranes as determined by one-way analysis of variance (ANOVA) with Tukey's multiple comparison test: mean difference, 95% CI of the difference, and adjusted P value In Graph Pad Prism 6 software, significant differences are indicated as follows: NS (not significant) P > 0.05, * P < 0.05, ** P < 0.01, *** P < 0.001 and **** P < 0.0001.

Comparison test	Mean Diff.	95% CI of diff.	Significant? P < 0.05?	Summary
TFC-20 vs. TFC-22.5	0.02317	-0.2627 to 0.3090	No	NS
TFC-20 vs. TFC-25	0.02009	-0.2657 to 0.3059	No	NS
TFC-22.5 vs. TFC-25	-0.003073	-0.2889 to 0.2827	No	NS

Table S12. Differences between contact angles of the TFC-20, TFC-22.5, and TFC-25 membranes as determined by one-way analysis of variance (ANOVA) with Tukey's multiple comparison test: mean difference, 95% CI of the difference, and adjusted P value In Graph Pad Prism 6 software, significant differences are indicated as follows: NS (not significant) P > 0.05, * P < 0.05, ** P < 0.01, *** P < 0.001 and **** P < 0.0001.

Comparison test	Mean Diff.	95% CI of diff.	Significant? P < 0.05?	Summary
TFC-20 vs. TFC-22.5	3.072	-0.8387 to 6.983	No	NS
TFC-20 vs. TFC-25	1.652	-2.259 to 5.563	No	NS
TFC-22.5 vs. TFC-25	-1.420	-5.331 to 2.491	No	NS

References

1. A. K. Ghosh and E. Hoek, Impacts of support membrane structure and chemistry on polyamide–polysulfone interfacial composite membranes, *J. Membr. Sci.*, 2009, **336**, 140-148.
2. J. Lee, J. H. Jang, H.-R. Chae, S. H. Lee, C.-H. Lee, P.-K. Park, Y.-J. Won and I.-C. Kim, A facile route to enhance the water flux of a thin-film composite reverse osmosis membrane: incorporating thickness-controlled graphene oxide into a highly porous support layer, *J. Mater. Chem. A*, 2015, **3**, 22053-22060.
3. J. E. Gu, S. Lee, C. M. Stafford, J. S. Lee, W. Choi, B. Y. Kim, K. Y. Baek, E. P. Chan, J. Y. Chung and J. Bang, Molecular Layer-by-Layer Assembled Thin-Film Composite Membranes for Water Desalination, *Adv. Mater.*, 2013, **25**, 4778-4782.
4. M. Hirose, H. Ito and Y. Kamiyama, Effect of skin layer surface structures on the flux behaviour of RO membranes, *J. Membr. Sci.*, 1996, **121**, 209-215.
5. S. H. Kim, S.-Y. Kwak and T. Suzuki, Positron annihilation spectroscopic evidence to demonstrate the flux-enhancement mechanism in morphology-controlled thin-film-composite (TFC) membrane, *Environ. Sci. Technol.*, 2005, **39**, 1764-1770.
6. M. T. M. Pendergast, J. M. Nygaard, A. K. Ghosh and E. M. Hoek, Using nanocomposite materials technology to understand and control reverse osmosis membrane compaction, *Desalination*, 2010, **261**, 255-263.
7. V. Lobo, Mutual diffusion coefficients in aqueous electrolyte solutions, *Pure Appl. Chem.*, 1993, **65**, 2613-2613.